

Answers to Anonymous Referee #2

We thank the anonymous referee #2 for his/her constructive comments and suggestions that certainly have improved the manuscript significantly. We revised the manuscript according to his/her comments and the comments of anonymous referees #1 and #3. In the following,

- *referee's comments are given in italic,*
- our answers are outlined in normal format, and
- **textual changes in the manuscript are given in bold format.**

General changes

We would like inform the anonymous referee #2 about the following changes:

1. Driven by the specific comment (SC) #18 of anonymous referee #3 (SC3.18), we decided to drop scenario S4 from the analysis. The difference between the sub-adiabatic model (S3) and the modified one (S4) is that the latter accounts for the depletion of the liquid water content due to entrainment, precipitation, and freezing drops. Consequently, we wanted to check whether S4 captures better the vertical stratification of the modeled low-level clouds and, accordingly, if it approximates the CREs of the reference simulation with better accuracy. Since S4 does not provide any further insight, we now have decided to drop this scenario. However, we do confirm that, by considering all the case days in the analysis, we came to the same conclusions as for 3 June. As a confirmation, we updated the Tables and attached them at the end of this document. The referee is referred to Tables R1–R3.
2. In all scenarios, we decided to drop sub-case d, which employs two fixed values for the droplet number concentration representing the two modes in the corresponding histogram for 3 June 2016. This scenario separates clouds into a cluster with low/high clouds. Considering the vertical variability of the droplet number concentration, the latter clustering will link low clouds (within the boundary layer) with high N_d and, accordingly, high clouds with lower N_d values. Thus, for all scenarios, employing such values for N_d are able to approximate the reference radiative transfer simulation very well. Only the radiative transfer simulation that is supplied by the droplet number concentration weighted over the cloud geometrical extent, i.e., N_{int} (sub-case b) leads to smaller differences when compared to the reference simulation. However, we do confirm that, by considering all the case days into the analysis, we came to the same conclusions as for 3 June. Note that, for the latter case, the clustering was conducted on the mean N_{int} over all case days. As a confirmation, we updated the Tables and attached them at the end of this document. The referee is referred to Tables R1–R3.
3. We decided to add a new scenario as a replacement of sub-case d, whereby radiative transfer simulations are conducted for a mean vertical profile of the droplet number concentration over all case days. Tables R9–R11 summarize the new results. In brief, this scenario is considered as an improvement compared to the clustering case. The following parts were included within the text:

Section 5.1.2: Last but not least, by replacing the vertical profile of N_d by the mean profile of N_d over all case days (see Fig. 2), emulates the cloud radiative effects of the reference simulation quite well. Accordingly, scenario S4 slightly undersimulates the mean SW CREs, with a mean error up to -3.16 W m^{-2} and a RMSE up to 17.2 W m^{-2} for both BOA and TOA. In fact, this scenario outperforms the rest scenarios (S1–S3), except from the sub-case b (N_{int}) in all scenarios. For an illustration of the excellent linear correlation between the reference simulation and S4 by means of a bivariate kernel density (BKD) plot, the reader is referred to Fig. B1 in Appendix B. One can see that the CREs computed by these scenarios are in a very good agreement almost everywhere except towards larger values of the CREs in case of the SW radiation, with Pearson correlations larger than 0.977 for both BOA and TOA.

Section 6: By employing a more representative profile for the N_d , i.e., a mean vertical profile of N_d over all case days leads to a rather good approximation; the RMSE is below 17.2 W m^{-2} . This points to the need to better account for prognostic N_d calculations.

Appendix B: In sect. 5.1.2, by conducting idealized radiative transfer simulations, we estimated the impact of the representation of cloud properties in ICON-LEM on the cloud radiative effects (CREs). Special emphasis was given on identifying the droplet number concentration (N_d), which approximates the microphysical and radiative properties of low-level clouds as simulated by ICON-LEM (reference scenario). A radiative transfer simulation, which employs a mean vertical profile of N_d over all the case days (scenario S4), approximates the CREs of the reference scenario quite well. Figure B1 depicts the excellent linear correlation between the reference simulation and S4 by means of a bivariate kernel density (BKD).

4. Following the general comment of anonymous referee #2 for shortening the manuscript given the redundancy of many of the results shown in this study and his/her relevant specific comments (SC), i.e., (SC2.12) and (SC2.25):
 - We decided to drop Fig. B1. Figure B1 illustrates the bivariate kernel density (BKD) between the cloud optical thickness and the liquid water path on a logarithmic scale. Considering the comprehensive explanation given in Sect. 3.3.1, we decided that this illustration did not provide any additional information.
 - Figures 6 and 7 have been revised. Now, they illustrate results only for TOA (see Figs R2 and R3).
 - We now focus only on the rotational component analysis. The mention of the principal component analysis have been significantly reduced. In addition, we removed the relevant information from Table 3. For the updated version of the Table, the referees are referred to Table R5. Additionally, we replaced Figure 5 by Table R4. This table lists the contribution of each rotational component to the total variance.

Answers to general comments (GC) from referee #2 (GC2)

(GC2.1) *There is already a significant body of work on the topic of sub-adiabaticity (much of which the authors cite) and the results of this study seem to confirm past findings (in particular, those of Merk et al., 2016) with little added insight into process (radiative, microphysical, etc.) besides pointing out that single-moment microphysics schemes leave much to be desired (which has been explored by e.g., Igel et al., 2015, JAS). Much work has also been done with respect to statistical emulators for understanding cloud radiative effects (e.g. Feingold et al., 2016; Glassmeier et al., 2019) and the aggregation of model data over all shallow cloudy columns severely limited the authors' ability to examine details regarding differences between cumulus and stratus (which likely exhibit very different fad), the diurnal cycle, or radiative effects across spatial scales – an exploration of the latter would be especially useful since the 300 m HOPE dataset is finer in horizontal resolution than the existing remote sensing products this study is designed to improve (typically 1 km pixel size).*

We acknowledge Referee's #2 concerns with respect to the novelty of this study. However, we respectfully disagree on this point. ICON-LEM domain consists of 150 vertical levels, with resolutions ranging from 25 m to 70 m within the boundary layer, from 70 m to 100 m further up to the altitude limit for the occurrence of low-level clouds selected for this study (4000 m), and from 70 m to 355 m further up until the top of the model domain at 21 km. This unprecedented high vertical resolution enables a significantly improved investigation of the vertical distribution of microphysical properties of low-level clouds as simulated by a double-moment scheme. We do agree that the vertical structure of adiabaticity depends on cloud regimes, types, and life-stage and, thus, it could be an interesting extension. However, due to the high horizontal resolution of ICON-LEM, for a single day, the number of "independent" cloudy columns are very large and complicates the investigation of such dependencies. Note here that the model output employed in this study, 3D HOPE data, has an output frequency of 15 min, while the domain size is limited to 45 km². For such studies, especially when it comes to life-stage, it would be better to use model data with higher output frequency, e.g., 1D profiles that are available every 10 sec. But, this is beyond the purpose of this study.

However, we revised our manuscript according to the comments of anonymous referees #1 and #3 and further extended our analysis to consider all case days to improve the robustness of our results. Now, sections 3.2 and 5 outline our findings for all case days.

(GC2.2) *Finally, I get the sense that this paper only deals with sub-adiabaticity in passing – the latter half of the paper is primarily concerned with describing CREs with a minimal set of variables and is almost completely disconnected from the title of the paper. Sub-adiabaticity seems to have only a weak influence on CREs.*

A high-resolution model as ICON-LEM is an ideal tool to investigate the suitability of the sub-adiabatic cloud model, firstly, for the evaluation of the representation of low-level clouds and, secondly, to capture the relevant properties which determine the cloud radiative effect. This outlines our main objectives and we think that it is reflected by the title of the paper.

We do not completely agree that the sub-adiabatic fraction has only a weak influence on the cloud radiative effect (CRE). In the first place, the sub-adiabatic fraction is the key component for

deriving the cloud optical thickness that is one of the fundamental cloud properties for describing the shortwave (SW) cloud radiative effects (CREs). Based on six case days, we found that the behavior of modeled liquid water clouds over Germany more closely resembles the sub-adiabatic model than the vertically homogeneous one, with a mean sub-adiabatic fraction (f_{ad}) of about 0.45. This model suggests, e.g., scaling of $\log(\tau)/\log(Q_L)$ with 5/6 and $f_{\text{ad}} < 1$. This scaling behavior has implications to, at least, the shortwave (SW) CRE. In addition, Eq. (15) contains the factor $\tau \propto f_{\text{ad}}^{-1/6}$. The latter factor, in combination with the mean sub-adiabatic fraction found in this study has a significant impact in τ compared to the pure adiabatic assumption that is usually employed.

Last but not least, the rotational component analysis (principal component and varimax rotation), clearly identifies the sub-adiabatic fraction as one of the minimal set of parameters to explain the CREs. In fact, it shows up as the 3rd rotational component (RC-3) that explains 14.8% of the total variance.

(GC2.3) *With respect to motivation, the authors rely heavily and repeatedly on the idea that there are large uncertainties in aircraft measurements of cloud drop number concentration (N_d in the authors' notation), which they justify by citing the N_d retrieval review paper of Grosvenor et al. (2018) – specifically, I believe they refer to Grosvenor et al.'s Figure 5 (which is in turn based on data used in Siebert et al., 2013) and accompanying discussion. This is an unfortunate figure. The disagreement of two probes (Phase Doppler Interferometer and Particulate Volume Monitor; PDI and PVM, respectively) at concentrations of $N_d > 350 \text{ cm}^{-3}$ is used as evidence that in situ probes have a general, systematic problem measuring N_d .*

The issue with this illustration is that one of the two probes used (PVM) is not designed to measure N_d and I am aware of no other publication in which this is even attempted. The PVM measures extinction from a population of cloud drops and makes no explicit count of particle density. In fact, I'm not even sure how this quantity was generated since the PVM returns only two data streams: total particle volume and surface area. The PDI, on the other hand, is frequently used by both the airborne cloud physics and industrial spray characterization communities and has been demonstrated to accurately count (and size) particles up to a concentration of $O(10^5) \text{ cm}^{-3}$. An intercomparison of PDI with other probes that explicitly count particles (CAS, FSSP, CDP, Holodec. . . etc. – there are a great number and I don't understand why Grosvenor et al. chose such an ill-suited probe for their figure) would likely show a much better overlap in the PDFs of N_d from different probes; such an intercomparison of the latest generation of cloud probes is currently underway for the recent NASA ORACLES campaign, which sampled a wide variety of concentration conditions due to the campaign's focus on interaction of clouds with overlying smoke layers during the stratocumulus to cumulus transition.

I am strongly opposed to the use of phrasing such as “large instrumental uncertainties” (e.g. page 23, lines 10-11) as I think this point is vastly overstated by Grosvenor et al. (2018), an assertion backed by their discussion of myriad other issues with retrieval assumptions ahead of any problems with in situ measurements.

We thank the anonymous referee #2 for the insight given. We revised this part of the text as follows:

The vertical variability of the droplet number concentration was examined. **For all the case days**, above an altitude of **about 2 km**, values of N_d are about 200 cm^{-3} and are, thus, close to climatological values, while in the boundary layer, the double moment scheme predicts N_d values above 600 cm^{-3} . Such values are **regarded as** rather high compared to satellite remote sensing estimates [1, 2], **but such comparison is rather vague considering, firstly, the large uncertainties of the satellite-derived estimates of cloud droplet number concentration [2] and, secondly, they are not available in high resolution.** However, in situ observations, **which are considered to be the most accurate approach to determine N_d ,** suggest higher values and, hence, lie closer to those simulated by ICON-LEM. **Thus, by means of in situ observations, evaluation activities should be conducted for a better characterization of the droplet number concentration from remote sensing techniques. The latter will scrutinize the double-moment scheme implemented in ICON-LEM and could potentially lead to better simulations of cloud processes and radiation.**

We additionally revised the corresponding text in Section 3.2 as follows,

On the contrary, in situ observations suggest higher values of N_d and, accordingly, closer to those simulated by ICON-LEM. **Hence, efforts should be undertaken to further validate the cloud droplet number concentrations predicted by the double-moment scheme.**

Answers to specific comments (SC) from referee #2 (SC2)

(SC2.1) P2, L7: *“taking placed” should be “taking place”*

The text is corrected.

(SC2.2) P2, L21-22: *“fixed droplet number distribution” – ambiguous terminology; “fixed droplet size distribution” would be clearer.*

The text is revised.

(SC2.3) P2, L23: *“Double-moment microphysical schemes... are only recently becoming more widespread”: Perhaps in the operational forecasting community this is true, but in research modeling (especially of warm clouds), double-moment schemes have been common for at least a decade.*

The referee is correct. We revised the text by adding at the end of the sentence: **in operational forecasting.**

(SC2.4) P5, L16: *Why do you use an indirect measure for rain/drizzle instead of directly examining rain water mixing ratio? I understand that it makes for a more straightforward comparison with observations, but it seems like an unnecessary step.*

The referee is correct. The reasoning was to perform a straightforward link to observations. However, we do consider the rain water content as an additional threshold. Relevant information

has been included.

(SC2.5) P6, L2: *“The model outputs the...”*

The text is revised.

(SC2.6) *Is the assumption of vertical homogeneity a “scheme?” Seems like an odd word choice.*

The text is revised accordingly and the word “scheme” is replaced by “model”.

(SC2.7) P7, L15: *“Clapeyron relationship”*

The word “relationship” has been included.

(SC2.8) P7, L16-17: *This sentence is difficult to follow. Rephrase and simplify the structure for clarity.*

The text is revised as follows: **For low level clouds, Γ_{ad} varies slightly ($\sim 20\%$). Consequently, in most studies, Γ_{ad} is assumed constant (e.g., Albrecht et al., 1990; Boers et al., 2006) or it is calculated from cloud bottom temperature and pressure (e.g., Merk et al., 2016) or cloud top information (e.g., Zeng et al., 2014).**

(SC2.9) P11, L8: *Remove “the” from “the 5 May...”*

The text is corrected.

(SC2.10) P13, L12-13: *“with a 5/6 slope” – possibly remove the word “fit,” doesn’t make sense in context.*

The text is revised accordingly.

(SC2.11) P13, L18: *If f_{ad} only accounts for 0.14% of the variance in τ , what’s the point of all this?*

Actually, in Sect. 3.3.1, we try to predict the cloud optical thickness derived from the output of ICON-LEM (by using Eq. 14), via employing the relevant equation suggested by the sub-adiabatic model, i.e., Eq. (15). Note here that, based on 6 case days, f_{ad} is 0.45 on average and not 1. For further information with respect to the relative importance of the sub-adiabatic fraction, the referee is referred to our answer at (GC2.2). This section has been revised:

Correction: f_{ad} accounts for 0.2% of the variance in τ .

With this intention, an effort has been conducted to predict the cloud optical thickness derived from Eq. (14) by employing the sub-adiabatic model and Eq. (15).

In fact, model $Y_4(Q_L, f_{\text{ad}}, N_{\text{int}})$ supports the applicability of the sub-adiabatic model since it is able to approximate the cloud optical thickness with high accuracy (RMSE =

0.027)

(SC2.12) *P13, Section 4: The step by step narrative of the PC analysis is overwrought. If you primarily intend to use the results of the RC analysis to justify the minimal set of variables needed to represent CREs, skip the PC discussion; the PC and RC results are sufficiently similar that it is redundant.*

We understand the referee's concerns, but we do not entirely agree that PC and RC results are sufficiently similar. Although each PC is clearly dominated by some properties, they are found moderately or strongly correlated with the remaining properties. On the contrary, the rotational component analysis points to exactly which properties dominate at each RC. However, we do agree that we provided a comprehensive analysis and, hence, we decided to revise and shorten the text. We now focus only on the rotational component analysis. The mention of the principal component analysis have been significantly reduced. In addition, we removed the relevant information from Table 3. For the updated version of the Table, the referee is referred to Table R5. Additionally, we replaced Figure 5 by Table R4. This table lists the contribution of each rotational component to the total variance.

(SC2.13) *P13, L34: "optimal" instead of "optimized"*

The text is corrected.

(SC2.14) *P14, Table 3 caption: Remove trailing zero from "moderate [0.40, 0.6]" for consistency*

The text is revised accordingly.

(SC2.15) *P14, L7-9: Rearrange sentence beginning "However, the PCs..." to simplify structure for clarity.*

The text is revised: However, the PCs are hard to interpret. **Although each new dimension is clearly dominated by some of the cloud properties, the PCs are found moderately or strongly correlated with other properties.**

(SC2.16) *P14, L11: remove "so-called" – this makes it look like other people have a different name for it.*

The word "so-called" has been removed.

(SC2.17) *P15, L9-10: I am confused by what you're doing here – are you always running multiple simulations, or for scenarios S2-S4 are you imposing LWC/ND profiles that are not actually from the simulations?*

We only conduct radiative transfer simulations. For the reference scenario, the input for the RRTMG was constructed on the basis of ICON-LEM. In other words, temperature, pressure, and water vapour profiles, surface temperature and pressure, and cloud liquid water content and droplet number concentration. In the rest scenarios (S1-S4), we preserve the liquid water content and the k_2 parameter (taken from ICON-LEM) and we vary only the droplet number concentration. In

addition, for scenarios S2-S4, the liquid water path for each profile is re-distributed over the vertical. In this way, we can estimate the effects of the bulk microphysical parameterizations and the vertical stratification of the cloud properties on the CREs. (The relevant information is found in sections 5.1 and 5.1.1).

(SC2.18) *P15-16, L33-3: the assumptions would be more clearly expressed in a table.*

A table listing the details of all the assumptions has been added according the referee’s suggestion (see Table R6).

(SC2.19) *P16, L1-2: Why are there drops in the free troposphere?*

It is true that aerosols and their precursor gases are mostly produced in the boundary layer. However, they can be transported into the free troposphere via different mechanisms, such as through convection and frontal uplift. There, their lifetime is much longer due to less efficient dry deposition as compared to the boundary layer and, accordingly, they can facilitate long-distance transport [3]. For example, Kupiszewski et al., (2013), reported that plumes in air aloft, above the boundary layer, can be attributed to transport of polluted air, e.g., via biomass burning. Biomass burning produces heat and moisture and this further leads to buoyancy-forced vertical and horizontal circulations of air and advection of hot gases [4]. The latter process is the main reason for the rapid uplift of smoke particles that are known to be an efficient CCN. Over the last decades, several studies reported aerosols in the free troposphere [5, 6] and even investigated CCN production there [7, 8, 9].

(SC2.20) *P16, L3: “where the liquid water path is preserved”*

The sentence is rearranged to be more clear: **Two different scenarios are considered, where the liquid water path is preserved within the vertical column, but the water content profile is redistributed.**

(SC2.21) *P16, L8: “following the climatology of a coarse. . .” – you only use the ECHAM value. Is this representative of what all GCMs do? If not, the generalization doesn’t work.*

The same droplet number concentration profile is adopted by the regional climate model REMO [10]. A similar climatology is employed by ICON-NWP, which is the global Numerical Weather Prediction (NWP) version of ICON model heinze2017. The only difference in ICON-NWP is that the droplet number concentration within the boundary layer is 200 cm^{-3} and not 220 cm^{-3} as in ECHAM and REMO. An example study, whereby the climatology of N_d implemented in ECHAM was compared to satellite retrieved N_d , is the one by Quaas et al., (2006). They retrieved N_d from MODIS and showed slightly lower values as compared to ECHAM N_d values, but consistent land-sea contrast [1].

The following part has been included in Section 3.1:

Note here that this value is close to the fixed droplet number concentration profile suggested by single-moment microphysical schemes adopted by atmospheric **models, such as ECHAM [11] and ICON-NWP, which is the global Numerical Weather Prediction (NWP) ver-**

sion of the ICON model [12].

(SC2.22) P17, Section 5.1.2: *I found the latter half of this discussion to be very difficult to follow, especially the references to various scenarios by only a letter or number near the end of the section (i.e. last paragraph, P18).*

We feel sorry for any inconvenience caused. The text has been revised.

(SC2.23) P18, Table 5 caption: *Cosine SZA was just given in text (and will hopefully be put in a separate table of assumptions) – remove since redundant.*

A table listing the details of all the assumptions has been added according the referee’s suggestion (see R6). Thus, we removed the aforementioned information from the caption of Table 5.

(SC2.24) P18, L1: *“and the rest of the simulated...”*

The text is revised accordingly.

(SC2.25) P19, Table 6: *Two things: 1) numbering of scenarios is off by one and 2) since BOA and TOA are almost always within 5% or 1 W/m² of each other, can you just pick one and reduce the amount of information here? This table would be much more effective/digestible.*

We thank the referee for highlighting the mistake in the numbering. We decided to keep the results for both BOA and TOA. However, we now have reduced the amount of scenarios employed in this study, hopefully making the table and the analysis easier to follow. In brief, we dropped scenario S4 (the modified sub-adiabatic mode), the sub-scenario (d, clusters), and included a new scenario representing the mean droplet number concentration profile over all case days. For a comprehensive description of all the changes made, the referee is referred to section **General changes** of the current document.

(SC2.26) P19, L11-14: *You can test whether effective radius is outside the range. Is this an issue or isn’t it?*

For all the scenarios, we inter-compared only columns with valid values for the effective radius. Thus, we revised the text as follows:

Note here that the RRTMG model is able to derive the radiative fluxes only for effective radius between 2.5 μm and 60 μm . **For all scenarios, all columns with effective radius outside this range have been excluded.**

(SC2.27) P20, Section 5.1.3: *As with the PCA results, what is the point of showing both correlations? You almost exclusively discuss Spearman, so why not just show that?*

We understand the referee’s concerns with respect to the use of both Spearman and Pearson correlations. The principal component analysis reveals systematic co-variations among the cloud properties. These components can be seen as a linear combination among the original properties and, hence, we employ the Pearson correlation to describe their relation. However, in Section

5.1.3, we describe the correlation between the cloud radiative effects and the cloud properties and the rotational components. In case of the SW radiation, Spearman correlation is the ideal metric to describe the monotonic relation between the CREs and the cloud optical thickness, liquid water path, and cloud geometrical extent (and, accordingly, RC-2). On the other hand, in the LW radiation, due to the linear relationship between the CREs and the cloud bottom and top heights (and, accordingly, RC-1), the right metric to describe their relation is the Pearson correlation. We decided to keep both correlations, but revised the text so that we highlight their importance.

(SC2.28) P20, L7: Capitalize “Spearman”

Corrected.

(SC2.29) P24, L3: *“uncover potential shortcomings in... models”: you only compared the model to itself, so how did you uncover shortcomings? Do you mean LES vs. GCM? Beyond discussing single- vs. double-moment microphysics (an already well-known issue), what shortcomings did you uncover?*

That was a mistake. We revised the text as follows: **The goal was ultimately to uncover potential shortcoming in the representation of clouds towards the computation of the cloud radiative effects.**

(SC2.30) P24, L11: *quantify contributions of 3rd/4th components to total variance here.*

We thank the referee for highlighting that we omitted an explicit reference to the contribution of the 3rd and 4th components to the total variance. These two components are clearly a function of the sub-adiabatic factor and the droplet number concentration (P20, L19), respectively, pointing to two clear degrees of freedom. They account for 14.8% and 13.6%, respectively, outlining their importance in identifying the minimum set of parameters for the representation of low-level clouds towards the computation of the CREs. Accordingly, we included the missing information. In addition, we decided to replace Figure 5 by a Table, where we list the contribution of each rotational component to the total variance.

(SC2.31) P24, L11: *delete “so-called”*

The word ”so-called” has been removed.

(SC2.32) P25, L9: *again, is the ECHAM climatological ND representative? Is it even backed by observations? You have not made a case for why this is a good number to use, besides the fact that a single GCM uses it.*

we addressed the latter issue in (SC.21).

(SC2.33) P25, L10: *How do two fixed values constitute a profile?*

The referee is correct. The use of the word “profile” for a constant droplet number concentration over the vertical can be misleading. We have removed the profile and replace it by the word “values” throughout the manuscript.

(SC2.34) P27, Eq A13: is exponent in denominator a typo? $D^0=1$.

Indeed there was a typo. The denominator is actually the zeroth moment of the droplet size distribution, which corresponds to the droplet number concentration. The text has been revised.

List of Figures

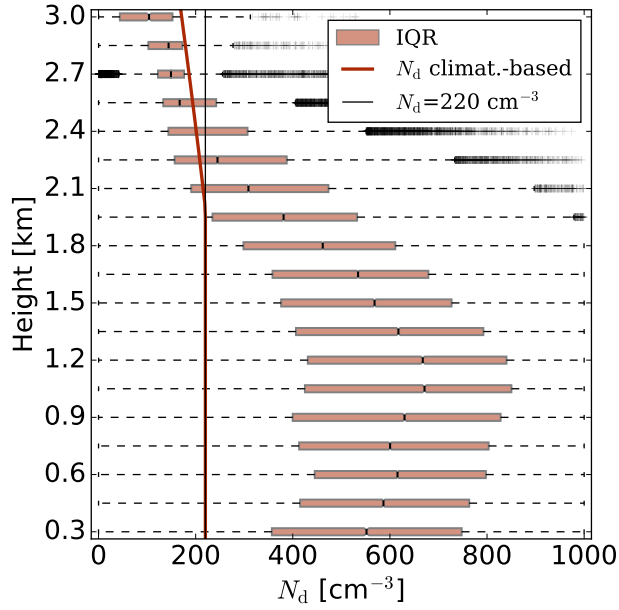


Figure R1: Box-whisker plot of the droplet number concentration for all the case days on average, describing the histograms of N_d simulated for different model levels by the double moment scheme of ICON-LEM. Boxes illustrate interquartile range (IQR), dark red line denotes the vertical N_d profile in case of the droplet number concentration employed in coarse climate models (climat.-based) and the thin black line demonstrates the constant N_d profile of 220 cm^{-3} .

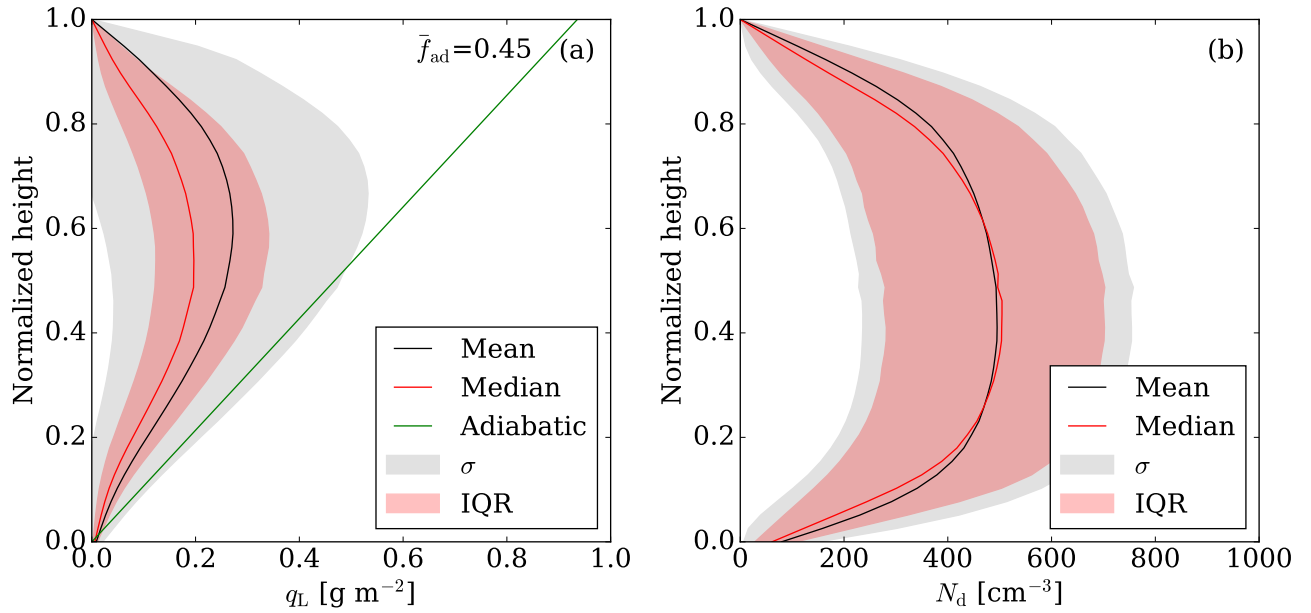


Figure R2: ICON-LEM simulated mean (a) q_L and (b) N_d profiles for all the case days on average. Profiles are normalized over height from the CBH to the CTH. Black lines denote the mean, red solid lines the median, gray shaded areas the standard deviation, red shaded areas the interquartile range (IQR), and the green solid line outline the mean adiabatic q_L profile characterized by a mean adiabatic fraction (\bar{f}_{ad}) of 0.45.

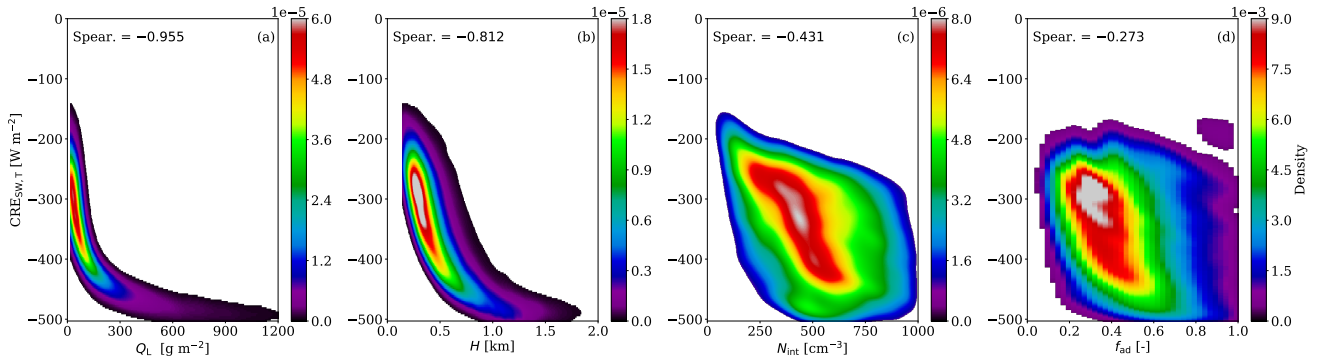


Figure R3: Bivariate kernel density (BKD) between the reference simulation (Ref.) and the cloud properties that are essential for the derivation of the cloud optical thickness that is one of the fundamental properties describing the SW cloud radiative effect. Panels illustrate the BKD between the $CRE_{SW,T}$ and (a) Q_L , (b) H , (c) N_{int} , and (d) f_{ad} . The corresponding Spearman (Spear.) correlations are highlighted.

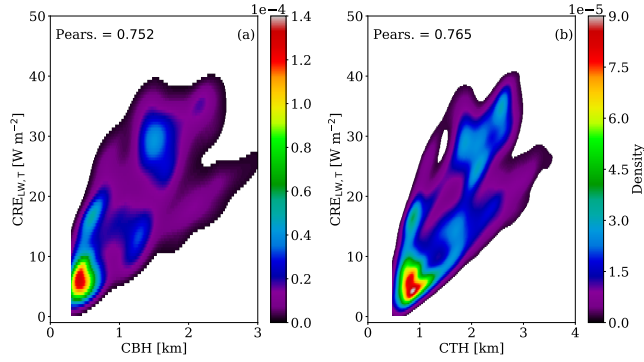


Figure R4: Bivariate kernel density (BKD) between the reference simulation (Ref.) and the cloud properties describing the LW cloud radiative effect at the BOA and (a) CBH and (b) CTH. The corresponding Pearson (Pears.) correlations are highlighted.

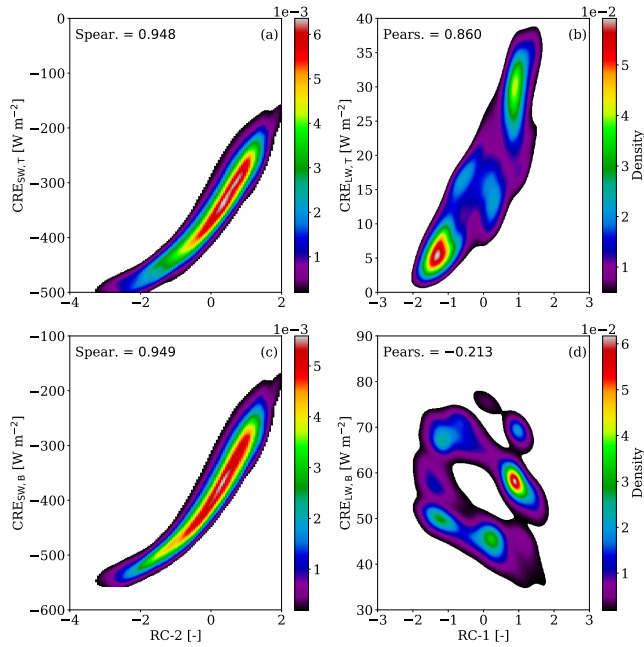


Figure R5: For the reference simulation (Ref.), bivariate kernel density (BKD) between CRE_{SW} and the second rotational component (RC-2) at (a) TOA, (c) BOA and between CRE_{LW} and the first rotational component (RC-1) at (b) TOA, (d) BOA. The corresponding Spearman (Spear.) and Pearson (Pears.) correlations are highlighted for the SW and LW radiation, respectively.

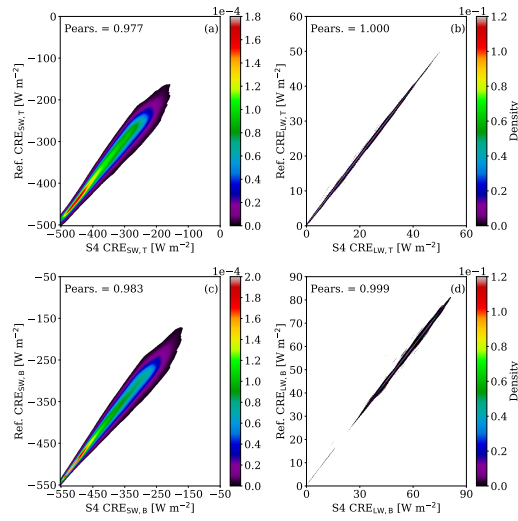


Figure R6: Bivariate kernel density (BKD) between the reference simulation (Ref.) and the scenario that employs the mean vertical N_d profile (S4). For the CREs, BKD are presented for the SW radiation at the TOA (a) and BOA (c), and for the LW radiation at the TOA (b) and BOA (d). The corresponding Pearson (Pears.) correlations are highlighted.

List of Tables

Table R1: Mean CRE (W m^{-2}) for the SW radiation. Results are given as differences between the new scenario minus the reference simulation (Δ). The root mean square error (RMSE) in W m^{-2} and the Pearson (Pears.) correlation between the new scenarios and the reference simulation are also given.

Scen.	$\text{CRE}_{\text{SW,B}}$			$\text{CRE}_{\text{SW,T}}$		
	Δ	RMSE	Pears.	Δ	RMSE	Pears.
S1a	-39.2	46.4	0.960	-40.1	47.0	0.952
S1b	-7.04	11.7	0.995	-6.53	11.7	0.994
S1c	-2.59	23.4	0.964	-1.86	24.3	0.951
S1d	-6.57	17.6	0.982	-5.99	18.0	0.977
S2a	-26.1	39.2	0.943	-27.1	39.8	0.930
S2b	7.74	14.2	0.991	8.19	13.6	0.990
S2c	12.9	32.4	0.943	13.7	33.6	0.921
S2d	8.53	22.6	0.971	9.10	22.9	0.964
S3a	-31.1	41.4	0.950	-32.9	42.9	0.937
S3b	1.47	10.6	0.993	1.17	10.0	0.992
S3c	6.59	27.7	0.953	6.55	29.0	0.934
S3d	2.29	19.1	0.976	2.09	19.5	0.969
S4a	-28.7	40.1	0.947	-30.3	41.4	0.934
S4b	4.97	11.7	0.993	4.80	11.1	0.992
S4c	10.1	29.9	0.949	10.2	31.2	0.928
S4d	5.72	20.4	0.975	5.67	20.8	0.967

Table R2: Mean CRE (W m^{-2}) for the LW radiation. Results are given as differences between the new scenario minus the reference simulation (Δ). The root mean square error (RMSE) in W m^{-2} and the Pearson (Pears.) correlation between the new scenarios and the reference simulation are also given.

Scen.	$\text{CRE}_{\text{LW,B}}$			$\text{CRE}_{\text{LW,T}}$		
	Δ	RMSE	Pears.	Δ	RMSE	Pears.
S1a	-0.11	0.48	0.999	-0.04	0.19	1.000
S1b	-0.05	0.40	0.999	-0.03	0.18	1.000
S1c	-0.01	0.50	0.999	-0.01	0.22	1.000
S1d	-0.04	0.45	0.999	-0.02	0.21	1.000
S2a	0.40	0.79	0.998	0.23	0.51	0.999
S2b	0.51	0.82	0.998	0.27	0.53	0.999
S2c	0.55	0.85	0.998	0.29	0.54	0.999
S2d	0.52	0.83	0.998	0.28	0.53	0.999
S3a	-0.05	0.74	0.997	0.33	0.64	0.999
S3b	-0.01	0.73	0.997	0.36	0.65	0.999
S3c	0.02	0.83	0.996	0.37	0.68	0.998
S3d	0.00	0.75	0.997	0.37	0.65	0.999
S4a	0.11	0.71	0.997	0.31	0.59	0.999
S4b	0.21	0.70	0.998	0.34	0.60	0.999
S4c	0.24	0.76	0.997	0.37	0.62	0.999
S4d	0.22	0.72	0.997	0.35	0.61	0.999

Table R3: Correlations between the cloud radiative effects and the cloud properties for the two major clusters characterized by low N_{int} values (L) and high N_{int} values (H). For the SW (LW) radiation, results are presented in case of the Spearman (Pearson) correlation.

Properties	$\text{CRE}_{\text{SW,B}}$		$\text{CRE}_{\text{SW,T}}$		$\text{CRE}_{\text{LW,B}}$		$\text{CRE}_{\text{LW,T}}$	
	L	H	L	H	L	H	L	H
Q_{L}	-0.935	-0.988	-0.930	-0.978	-0.016	-0.309	0.216	0.303
τ	-0.992	-0.994	-0.983	-0.986	0.028	-0.324	0.195	0.291
N_{int}	-0.446	-0.128	-0.410	-0.105	0.419	0.202	-0.259	-0.067
r_{int}	-0.343	-0.867	-0.353	-0.854	-0.311	-0.365	0.323	0.268
CBH	0.143	-0.213	-0.057	-0.292	-0.311	-0.239	0.752	0.786
CTH	-0.122	-0.604	-0.201	-0.663	-0.302	-0.376	0.783	0.717
H	-0.776	-0.921	-0.787	-0.925	-0.024	-0.386	0.217	0.300
f_{ad}	-0.126	-0.271	-0.129	-0.256	-0.003	0.144	0.215	0.194

Table R4: Explained variance and cumulative explained variance from different components obtained by the rotational component analysis (RC).

	RC-1	RC-2	RC-3	RC-4	RC-5	RC-6	RC-7	RC-8	RC-9
Explained variance (%)	33.8	35.5	14.8	13.6	2.10	0.10	0.10	0.00	0.00
Cumulative proportion (%)	33.8	69.3	84.1	97.7	99.8	99.9	100	100	100

Table R5: Pearson correlations between the logarithm of the cloud properties and the rotational components (RC). Degree of correlation (absolute values): (a) very weak: below 0.2, (b) weak: [0.2, 0.4), (c) moderate: [0.4, 0.6), (d) strong: [0.6, 0.8), and (e) very strong [0.8, 1.0].

Properties	RC-1	RC-2	RC-3	RC-4
CBH	0.969	0.025	-0.001	0.201
CTH	0.919	-0.282	0.076	0.237
Γ_{ad}	-0.896	-0.014	0.073	-0.183
τ	-0.062	-0.971	-0.192	-0.125
Q_{L}	0.036	-0.968	-0.240	0.052
H	0.177	-0.937	0.285	0.094
f_{ad}	-0.010	-0.099	-0.995	-0.025
N_{int}	-0.518	-0.250	-0.244	-0.778
r_{int}	0.382	-0.536	-0.314	0.681

Table R6: Input parameters for the RRTMG model.

Parameter	Value
Cosine of solar zenith angle	0.70
Carbon dioxide concentration	399 ppm
Ultraviolet/Visible surface albedo for direct radiation	0.05
Ultraviolet/Visible surface albedo for diffuse radiation	0.05
Near-infrared surface albedo for direct radiation	0.30
Near-infrared surface albedo for diffuse radiation	0.30

Table R7: Simulated scenarios. For scenarios S1–S3, three individual simulations (sub-cases) have been conducted according to different values for the droplet number concentration.

Scenarios			
Ref.	Double-moment scheme		
S1	Single-moment scheme		
S2	Vertical homogeneous model		
S3	Sub-adiabatic model		
S4	Mean vertical N_{d} profile		
Sub-cases	a. 220 cm^{-3}	b. N_{int}	c. 480 cm^{-3}

Table R8: Mean and standard deviation of modeled CREs (W m^{-2}) for the SW, LW, and NET (SW + LW) radiation for the reference simulation over all case days. ATM stands for the atmospheric cloud radiative effect defined as the difference between the CREs at the TOA and BOA.

Ref.	CRE_{SW}	CRE_{LW}	CRE_{NET}
TOA	-348.7 ± 78.39	17.51 ± 10.04	-331.2 ± 77.27
ATM	32.94 ± 12.11	-39.16 ± 13.14	-6.225 ± 12.98
BOA	-381.6 ± 86.95	56.66 ± 9.746	-324.9 ± 86.51

Table R9: Mean CRE (W m^{-2}) for the SW radiation. Results are given as differences between the new scenario minus the reference simulation (Δ). The root mean square error (RMSE) in W m^{-2} and the Pearson (Pears.) correlation between the new scenarios and the reference simulation are also given.

Scen.	CRE _{SW,B}			CRE _{SW,T}		
	Δ	RMSE	Pears.	Δ	RMSE	Pears.
S1a	-39.2	46.4	0.960	-40.1	47.0	0.952
S1b	-7.04	11.7	0.995	-6.53	11.7	0.994
S1c	-2.59	23.4	0.964	-1.86	24.3	0.951
S2a	-26.1	39.2	0.943	-27.1	39.8	0.930
S2b	7.74	14.2	0.991	8.19	13.6	0.990
S2c	12.9	32.4	0.943	13.7	33.6	0.921
S3a	-31.1	41.4	0.950	-32.9	42.9	0.937
S3b	1.47	10.6	0.993	1.17	10.0	0.992
S3c	6.59	27.7	0.953	6.55	29.0	0.934
S4	-3.13	16.7	0.983	-3.16	17.2	0.977

Table R10: Correlations between the cloud radiative effects for the reference simulation (Ref.) and the cloud properties. For the SW (LW) radiation, results are presented in case of the Spearman (Pearson) correlation.

Properties	CRE _{SW,B}	CRE _{SW,T}	CRE _{LW,B}	CRE _{LW,T}
	Spearman		Pearson	
Q_L	-0.957	-0.955	-0.129	0.181
τ	-0.994	-0.987	0.104	0.148
N_{int}	-0.471	-0.431	0.428	-0.290
r_{int}	-0.446	-0.460	-0.395	0.344
CBH	0.148	0.063	-0.389	0.752
CTH	0.143	-0.220	-0.428	0.765
H	-0.795	-0.812	-0.200	0.226
f_{ad}	-0.284	-0.273	0.145	0.134

Table R11: Mean CRE (W m^{-2}) for the LW radiation. Results are given as differences between the new scenario minus the reference simulation (Δ). The root mean square error (RMSE) in W m^{-2} and the Pearson (Pears.) correlation between the new scenarios and the reference simulation are also given.

Scen.	$\text{CRE}_{\text{LW,B}}$			$\text{CRE}_{\text{LW,T}}$		
	Δ	RMSE	Pears.	Δ	RMSE	Pears.
S1a	-0.11	0.48	0.999	-0.04	0.19	1.000
S1b	-0.05	0.40	0.999	-0.03	0.18	1.000
S1c	-0.01	0.50	0.999	-0.01	0.22	1.000
S2a	0.40	0.79	0.998	0.23	0.51	0.999
S2b	0.51	0.82	0.998	0.27	0.53	0.999
S2c	0.55	0.85	0.998	0.29	0.54	0.999
S3a	-0.05	0.74	0.997	0.33	0.64	0.999
S3b	-0.01	0.73	0.997	0.36	0.65	0.999
S3c	0.02	0.83	0.996	0.37	0.68	0.998
S4	-0.02	0.49	0.999	-0.02	0.22	1.000

References

- [1] J. Quaas, O. Boucher, and U. Lohmann, “Constraining the total aerosol indirect effect in the lmdz and echam4 gcms using modis satellite data,” *Atmos. Chem. Phys.*, vol. 6, no. 4, pp. 947–955, 2006.
- [2] D. P. Grosvenor, O. Sourdeval, P. Zuidema, A. Ackerman, M. D. Alexandrov, R. Bennartz, R. Boers, B. Cairns, J. C. Chiu, M. Christensen, H. Deneke, M. Diamond, G. Feingold, A. Fridlind, A. Hünerbein, C. Knist, P. Kollias, A. Marshak, D. McCoy, D. Merk, D. Painemal, J. Rausch, D. Rosenfeld, H. Russchenberg, P. Seifert, K. Sinclair, P. Stier, B. van Diedenhoven, M. Wendisch, F. Werner, R. Wood, Z. Zhang, and J. Quaas, “Remote sensing of droplet number concentration in warm clouds: A review of the current state of knowledge and perspectives,” *Rev. Geophys.*, vol. 56, no. 2, pp. 409–453, 2018.
- [3] S. Zhou, S. Collier, D. A. Jaffe, and Q. Zhang, “Free tropospheric aerosols at the mt. bachelor observatory: more oxidized and higher sulfate content compared to boundary layer aerosols,” *Atmos. Chem. Phys.*, vol. 19, no. 3, pp. 1571–1585, 2019.
- [4] P. Kupiszewski, C. Leck, M. Tjernström, S. Sjogren, J. Sedlar, M. Graus, M. Müller, B. Brooks, E. Swietlicki, S. Norris, and A. Hansel, “Vertical profiling of aerosol particles and trace gases over the central arctic ocean during summer,” *Atmos. Chem. Phys.*, vol. 13, no. 24, pp. 12405–12431, 2013.
- [5] R. J. Weber and P. H. McMurry, “Fine particle size distributions at the mauna loa observatory, hawaii,” *J. Geophys. Res. Atmos.*, vol. 101, no. D9, pp. 14767–14775, 1996.
- [6] A. L. Igel, A. M. L. Ekman, C. Leck, M. Tjernström, J. Savre, and J. Sedlar, “The free troposphere as a potential source of arctic boundary layer aerosol particles,” *Geophys. Res. Lett.*, vol. 44, no. 13, pp. 7053–7060, 2017.

- [7] G. C. Roberts, D. A. Day, L. M. Russell, E. J. Dunlea, J. L. Jimenez, J. M. Tomlinson, D. R. Collins, Y. Shinozuka, and A. D. Clarke, “Characterization of particle cloud droplet activity and composition in the free troposphere and the boundary layer during intex-b,” *Atmos. Chem. Phys.*, vol. 10, no. 14, pp. 6627–6644, 2010.
- [8] F. Bianchi, J. Tröstl, H. Junninen, C. Frege, S. Henne, C. R. Hoyle, U. Molteni, E. Herrmann, A. Adamov, N. Bukowiecki, X. Chen, J. Duplissy, M. Gysel, M. Hutterli, J. Kangasluoma, J. Kontkanen, A. Kürten, H. E. Manninen, S. Münch, O. Peräkylä, T. Petäjä, L. Rondo, C. Williamson, E. Weingartner, J. Curtius, D. R. Worsnop, M. Kulmala, J. Dommen, and U. Baltensperger, “New particle formation in the free troposphere: A question of chemistry and timing,” *Science*, vol. 352, no. 6289, pp. 1109–1112, 2016.
- [9] C. Rose, K. Sellegri, I. Moreno, F. Velarde, M. Ramonet, K. Weinhold, R. Krejci, M. Andrade, A. Wiedensohler, P. Ginot, and P. Laj, “Ccn production by new particle formation in the free troposphere,” *Atmos. Chem. Phys.*, vol. 17, no. 2, pp. 1529–1541, 2017.
- [10] J.-P. Pietikäinen, T. Markkanen, K. Sieck, D. Jacob, J. Korhonen, P. Räisänen, Y. Gao, J. Ahola, H. Korhonen, A. Laaksonen, and J. Kaurola, “The regional climate model remo (v2015) coupled with the 1-d freshwater lake model flake (v1): Fenno-scandinavian climate and lakes,” *Geosci. Model Dev.*, vol. 11, no. 4, pp. 1321–1342, 2018.
- [11] M. Giorgetta, E. Roeckner, T. Mauritsen, J. Bader, T. Crueger, M. Esch, S. Rast, L. Kornblueh, H. Schmidt, S. Kinne, C. Hohenegger, B. Möbis, T. Krismer, K.-H. Wieners, and B. Stevens, “The atmospheric general circulation model echam6 - model description,” *Max-Planck-Institut für Meteorologie*, vol. 135, 01 2013.
- [12] R. Heinze, A. Dipankar, C. C. Henken, C. Moseley, O. Sourdeval, S. Trömel, X. Xie, P. Adamidis, F. Ament, H. Baars, C. Barthlott, A. Behrendt, U. Blahak, S. Bley, S. Brdar, M. Brueck, S. Crewell, H. Deneke, P. Di Girolamo, R. Evaristo, J. Fischer, C. Frank, P. Friederichs, T. Göcke, K. Gorges, L. Hande, M. Hanke, A. Hansen, H.-C. Hege, C. Hoose, T. Jahns, N. Kalthoff, D. Klocke, S. Kneifel, P. Knippertz, A. Kuhn, T. van Laar, A. Macke, V. Maurer, B. Mayer, C. I. Meyer, S. K. Muppa, R. A. J. Neggers, E. Orlandi, F. Pantillon, B. Pospichal, N. Röber, L. Scheck, A. Seifert, P. Seifert, F. Senf, P. Siligam, C. Simmer, S. Steinke, B. Stevens, K. Wapler, M. Weniger, V. Wulfmeyer, G. Zängl, D. Zhang, and J. Quaas, “Large-eddy simulations over germany using icon: a comprehensive evaluation,” *Q. J. R. Meteorol. Soc.*, vol. 143, no. 702, pp. 69–100, 2017.